Journal of Biomechanics 42 (2009) 319–324

Contents lists available at ScienceDirect

Journal of Biomechanics

journal homepage: www.elsevier.com/locate/jbiomech
www.JBiomech.com

Prediction of joint center location by customizable multiple regressions: Application to clavicle, scapula and humerus

V. Sholukha[a,b,*], S. Van Sint Jan[a], O. Snoeck[a], P. Salvia[a], F. Moiseev[a,b], M. Rooze[a]

[a] Laboratory of Anatomy, Biomechanics and Organogenesis (LABO), Université Libre de Bruxelles (ULB), Faculty of Medicine, Belgium
[b] Department of Applied Mathematics, Polytechnical University, Saint Petersburg, Russia

ARTICLE INFO

Article history:
Accepted 13 November 2008

Keywords:
Multiple regression
Joint center
Scapula
Humerus
Clavicle
Bone morphology
Palpation

ABSTRACT

Accurate spatial location of joint center (JC) is a key issue in motion analysis since JC locations are used to define standardized anatomical frames, in which results are represented. Accurate and reproducible JC location is important for data comparison and data exchange. This paper presents a method for JC locations based on the multiple regression algorithms without preliminary assumption on the behavior of the joint-of-interest. Regression equations were obtained from manually palpable ALs on each bone-of-interest. Results are presented for all joint surfaces found on the clavicle, scapula and humeral bone. Mean accuracy errors on the JC locations obtained on dry bones were 5.2 ± 2.5 mm for the humeral head, 2.5 ± 1.1 mm for the humeral trochlea, 2.3 ± 0.9 mm for the humeral capitulum, 8.2 ± 3.9 mm for the scapula glenoid cavity, 7.2 ± 3.2 mm for the scapular aspect of the acromio-clavicular joint, 3.5 ± 1.8 mm for the clavicular aspect of the sternoclavicular joint and 3.2 ± 1.4 mm for the clavicular aspect of the acromio-clavicular joint. In-vitro and in-vivo validation accuracy was 5.3 and 8.5 mm, respectively, for the humeral head center location. Regression coefficients for joint radius dimension and joint surface orientation were also processed and reported in this paper.

1. Introduction

Spatial location of anatomical landmarks (ALs) is often required to quantify various aspects of skeletal morphology. ALs are required to define anatomical frames to represent movement data according to conventions (Cappozzo et al., 2005). Most ALs can be located either by manual palpation or virtual palpation on three-dimensional (3D) models, or a combination of both (Van Sint Jan et al., 2006; Van Sint Jan, 2007). Key ALs like joint center (JC) positions are required to meet standards (Wu and Cavanagh, 1995; Wu et al., 2002, 2005) and are not palpable. Despite their usefulness, previously published methods use to estimate JCs show shortages. Functional methods are recognized to be the most accurate method (Stokdijk et al., 2000). They use particular movements to determine mechanical JCs and seem satisfactory for ball-and-socket joints in normal conditions (Camomilla et al., 2006; Cappozzo, 1984; Leardini et al., 1999). Unfortunately, they require performing motion patterns that are often too complex for patients showing limited joint amplitude (Di Silvestro et al., 2007). Morphological methods use spatial locations of palpable ALs to determine JCs using regression analysis (Barbaix et al., 2000; Bell et al., 1990; Meskers et al., 1998). Morphological methods seem therefore more appropriate because the analyzed individual patient can remain at rest during the palpation. To allow reproducible JC construction, ALs must lie close to the skin surface to be relatively accessible to palpation and must be readily identifiable even by less experienced investigators. Past effort developed strict AL definition to improved AL palpation reproducibility (Van Sint Jan, 2007). Recent findings reported that manual palpation of the humerus and scapula ALs can be achieved with a satisfactory accuracy (Van Sint Jan et al., 2007). For the shoulder complex, some morphological methods assume that the scapula glenoid cavity and the humeral head share the same center (Barbaix et al., 2000; Bell et al., 1989, 1990; Meskers et al., 1998). In such method, the shoulder JC is determined from scapula ALs. This seems acceptable for shoulder joints showing normal behavior, but less acceptable for pathological instable joints (Grant et al., 2007). In such conditions, one cannot assume that the relationships between scapular ALs and the humeral head center remain constant during movements occurring in the glenohumeral joint (Yamamoto et al., 2007). Some authors reported that the glenohumeral joint does not behave like a pure ball-and-socket joint in normal conditions, and that physiological laxity is observable (Hatzel et al., 2006). This contradicts the above equivalence assumption. Joint size estimation is also of interest for arthroplasty (Harryman et al., 1995).

This study aimed to determine if the position of the morphological shoulder JCs can be interpolated with satisfactory

* Corresponding author at: Universite Libre De Bruxelles (ULB), Faculte De Medicine Et De Pharmacie, Lab. D'Anatomie and Organogenesis (LABO), Route de Lennik, 808 - CP 619, 1070 Brussel, Belgium. Tel.: +32 2 555 6262; fax: +32 2 555 6378.
E-mail address: vcholouk@ulb.ac.be (V. Sholukha).

0021-9290/$ - see front matter © 2008 Elsevier Ltd. All rights reserved.
doi:10.1016/j.jbiomech.2008.11.004

accuracy from enough ALs palpated on the bone-of-interest itself. This statement was made possible after the availability of detailed palpation definitions of skeletal ALs (Van Sint Jan, 2007). Such standardized AL definitions allowed increasing palpation repeatability (Van Sint Jan and Della Croce, 2005). Results, including in-vitro and in-vivo validation, for the shoulder joint complex bones are presented. The main goal of this paper was obtaining regression relationships applicable for in-vivo shoulder motion analysis. This method would allow estimating patient's joint surface center, orientation and dimensions without a-priori knowledge on the functional aspect of the joint. The method was then compared with other morphological methods applied on the shoulder (Meskers et al., 1998).

2. Material and methods

2.1. Anatomical landmarks and palpation

Dry bones (78 humerus [42 Left, 36 Right], 57 scapula [36L, 21R], 44 clavicle [26L, 18R]) from the ULB osteology collection were available. All left/right bones were obtained from different specimens. No difference between right and left bones were made. Specimen gender was not available. Each bone was firmly attached to the experimental bench to avoid artefacts due to displacement between bone and digitizer. All landmarks used in this paper were readily palpable (Van Sint Jan, 2007) (Fig. 1). Some of these ALs (for the humerus: 5, 7 and GH; for the scapula: 1, 2, 4 and 7) are recommended by the ISB (Wu et al., 2005). For each bone, AL spatial coordinates and joint surfaces (Fig. 1) were digitized using a 3D digitizer (Platinum FaroArm© 4ft., constructor accuracy = 0.013 mm). All ALs were defined in the digitizer global frame. Joint surfaces were digitized by taking points (between 15 and 30 points depending of the surface) evenly distributed (Fig. 1). The humeral trochlea was digitized by taking five evenly distributed points along its groove (Fig. 1d). Further data processing allowed performing linear and spherical approximations of the digitized surfaces (Table 1).

2.2. Data approximation

2.2.1. Building the local frames

For each bone, several local coordinate systems (CSs) were created using all possible combinations of digitized ALs to estimate the three orthogonal CS axes accurately. The best AL combinations have been determined using leave-one-out cross-validation error (LOO-XVE) (Ripley, 1996) and are presented. Following Meskers et al.'s suggestion (Meskers et al., 1998), results from left bones were mirrored.

2.2.1.1. Humerus technical frame. The local CS of each humerus was built.

Let us assume G_i, $i=\overline{1,7}$ (i = AL index, see Fig. 1) as vector columns $G_i=(G_{ix},G_{iy},G_{iz})^T$ corresponding to the seven digitized humeral AL locations defined in the global CS.

Let us define $G_t=(G_5+G_7)/2$.

Three different local CS$_j$ were tested from a subset G_j (j = 1, 2, or 3), and according to orts $Y_j=[|G_j-G_t|]$, where $[|P|]=P/\|P\|$, $P=(P_x,P_y,P_z)^T$ and $\|P\|$ is norm of the vector column of point P.

Let us then define the scalars $C_j=Y_j^T(G_7-G_t)$.

The origin of the humerus local CS$_j$ was therefore defined as $G_{0j}=C_jY_j+G_t$.

Further, the Z-axis was given by orts $Z_j=[|G_7-G_{0j}|]$.

Finally, X-axis was found by the cross product orts $X_j=\tilde{Y}_jZ_j$, where $\tilde{P}=\begin{bmatrix}0 & -P_z & P_y\\ P_z & 0 & -P_x\\ -P_y & P_x & 0\end{bmatrix}$.

In order to define the ALs in the new CS$_j$, let define the rotation $R_j=(X_j,Y_j,Z_j)$.

Then, we obtained the vector columns

$$L_{ij}=R_j^T(G_i-G_{0j}),\quad i=\overline{1,7},\quad j=1,2,3, \tag{1}$$

where L_{ij} are the ALs in local CSs.

2.2.1.2. Scapula technical frame. The local CS of each scapula was built in a similar way than for the humerus. Using a similar designation with the eight available

Table 1
Scalar and vector parameters approximated in this study.

Humerus	Scapula	Clavicle
Head (I): 3D, *R* Trochlea (VI): 3D, *N* Capitulum (VII): 3D, *R*	Glenoid cavity (II): 3D, *R* AC (V): 3D, *N*	SC (III): 3D, *N* AC (IV): 3D, *N*

3D = spatial coordinates of morphological joint center. R = radius of surface (when spherical). N = normal to joint surface (when not spherical). Each column shows anatomical features that have been analyzed for a particular bone. Roman numbers indicate the joint surfaces shown in Fig. 1.

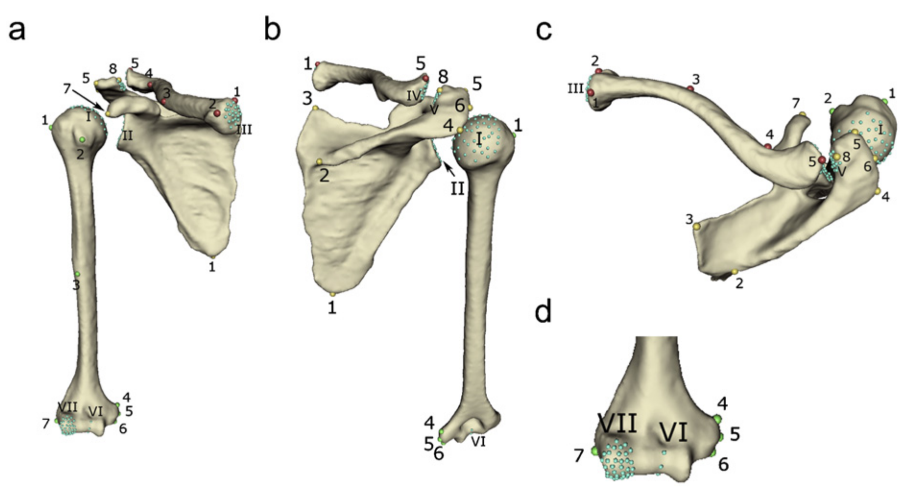

Fig. 1. Anatomical features digitized in this study (illustrated on the 3D models obtained from the specimen used for the in-vitro validation study; joint spaces have been virtually slightly opened to better show the joint surface). (a) Anterior view, (b) posterior view, (c) superior view and (d) anterior view of the distal humerus epiphysis. The following landmarks have been located and processed for JC interpolation (AL index are also used in the equations of this paper). Humerus: greater tubercle (HGT, 1), lesser tubercle (HLT, 2), deltoid tuberosity (HDT, 3), upper angle of medial epicondyle (HMU, 4), center of medial epicondyle (HME, 5), lower angle of the medial epicondyle (HML, 6), lateral epicondyle (HLE, 7). Scapula: inferior angle (SIA, 1), root of spine (SRS, 2), superior angle (SSA, 3), acromial angle (SAA, 4), acromial tip (SAT, 5), acromial edge (SAE, 6), coracoid tip (SCT, 7), upper edge of acromioclavicular joint—(SAJ, 8). Clavicle: upper edge of sternoclavicular joint (CSJ, 1), anterior edge of sternoclavicular joint (CAS, 2), anterior convexity (CAE, 3), anterior concavity (CAA, 4), upper edge of acromioclavicular joint (CAJ, 5). The following joint surfaces have been digitized as well. For the glenohumeral (GH) *joint*: humeral head (I) and scapula glenoid cavity (II). For the sterno-clavicular (SC) joint: sternal joint surface of the clavicle (III). For the acromio-clavicular (AC) joint: acromial surface of the clavicle (IV) and the clavicular surface of the scapula (V). For the humero-ulnar (HU) joint: humeral trochlea groove (VI). For the humero-radial joint (HR): humeral capitulum (VII).